



Repositorio Institucional de la Universidad Autónoma de Madrid

<https://repositorio.uam.es>

Esta es la **versión de autor** del artículo publicado en:
This is an **author produced version** of a paper published in:

VACUUM 150 (2018): 232-238

DOI: <http://doi.org/10.1016/j.vacuum.2018.01.045>

Copyright: © 2018 Elsevier Ltd.

El acceso a la versión del editor puede requerir la suscripción del recurso
Access to the published version may require subscription

Biofunctional porous silicon micropatterns engineered through visible light activated epoxy capping and selective plasma etching

C. Rodríguez¹, O. Ahumada³, V. Cebrián³, V. Torres Costa^{1,2}, M. Manso Silván^{1*}

¹Departamento de Física Aplicada and Instituto de Ciencia de Materiales Nicolás Cabrera, Universidad Autónoma de Madrid, 28049, Madrid, Spain

²Centro de Microanálisis de Materiales, Universidad Autónoma de Madrid, 28049, Madrid, Spain

³Mecwins, Tres Cantos, 28760 Madrid, Spain

*corresponding author: miguel.manso@uam.es, tel: +34 914974918

Abstract

Porous silicon (PSi) is a versatile matrix with tailorable surface reactivity, which allows processing a diversity of biofunctional structures. An assembly process has been activated by catalyzing PSi oxidation with visible light, enabling subsequent binding with (3-glycidyloxypropyl)-trimethoxy-silane (GPTMS) in the submonolayer regime. A multispectroscopic approach has been followed to fully characterize the surface capped PSi. XPS has been used to trace the process of light induced oxidation and GPTMS assembly on supported PSi. Field emission SEM confirms that the surface topography is not modified by the activated assembly. To complement the chemical analysis of the bound GPTMS, FTIR and solid state NMR were used on functionalized PSi particles. Finally, the surfaces of GPTMS capped PSi have been successfully micropatterned by a masked Ar plasma etching process. The process gives rise to surface hydrophilic/hydrophobic contrasts, which are efficient in the selective binding of activated gold nanoparticles. The contrasts were applied to the local recognition of mouse serum proteins adsorbed on GPTMS functionalized PSi through an immunofluorescence assay. The results confirm the effectiveness of GPTMS capped PSi as adsorptive layer for immunosensing.

Keywords: porous silicon, organosilanes, biofunctional particles, solid state NMR, surface functionalization

1. Introduction

Functionalization of semiconductor nanostructures with organic monolayers is an attractive process that can serve to make the properties of the original semiconductor compatible with a tailored surface chemistry [1,2]. Nanostructured porous Silicon (PSi) can be described as a matrix of silicon quantum dots immersed in an amorphous Si/silica network. PSi is an extremely versatile material which allows control over its pore structure leading to high specific surface areas (hundreds of m^2/g) [3]. PSi is generally bioengineered on a supported Si wafer [4], but has been described also in the form of particles in a wide range of applications [5]. The pore structure and porosity of PSi can be adapted depending on the specific envisaged application. Although both micro- and mesopores can be used to achieve high porosity, mesoporous structures are generally preferred because they exhibit better mechanical stability in comparison to the microporous ones [6]. Furthermore, the pores present an open structure and are accessible to biomolecules such as enzymes, which enables its biocatalytic functionalization [7].

Besides, the controlled surface reactivity of PSi opens new opportunities to tune the material for specific biomedical applications [8]. Assembly has been previously proposed by visible light activated hydrosilylation (reaction between hydrogen-terminated silicon and molecules containing double bonds) [9,10] but surface modification with organosilane assemblies allows diversifying the chemical functionalities and provides biomolecular selectivity [11]. Relevantly, the assembly of organosilanes on PSi surfaces requires a previous oxidation that has been traditionally promoted by thermal process or peroxidation [12]. Relevantly, recent reports have demonstrated that oxidation of PSi can be catalyzed upon exposure to visible light, leading to an increase of free electrons at the PSi interface, which can efficiently reduce metals [13]. Here we propose that the electron density induced upon light activation can catalyze the heterogeneous condensation reactions of (3-glycidyoxy-propyl)-

trimethoxy-silane (GPTMS) with the surface of the oxidized PSi, avoiding previous thermal or chemical oxidation [12]. Epoxy groups in GPTMS are able to react with different nucleophilic groups providing strong linkages not drastically altering protein function [14], which is exploited to develop protocols for enzyme immobilization.

Plasma processes have been extensively used for biofunctionalization purposes in a diversity of configurations. The most extended mode, plasma polymerization (an alternative name for plasma enhanced chemical deposition of strictly organic monomers) has been used for deposition of amines [15,16], carboxylic acid [17,18] and other chemical functionalities. However, this process is not compatible with the epoxy group, very unstable face to ionic, electronic and radiative activation in the plasma. The alternative to this process has been a previous plasma activation of the target substrate and an ulterior reaction with a glycidyl monomer (plasma grafting process) [19]. In spite of the demonstrated functionality in adhesion applications, the grafting of these epoxy functionalities is more often performed by radiation induced (UV) activation, allowing a selective patterning of the surface [20]. This process is however not straightforward with the silane chemistry, in view of the low partial pressure of the epoxy silane precursors at typical thermodynamic conditions. Selective plasma etching, a process carried out under partial masking of the surface, appears as the most attractive way to micropattern organosilane functionalized surfaces for traditional microelectronic [21] or biomedical applications [22].

In this work, we aim at studying the visible light activated surface functionalization of PSi with one of the most common epoxy silanes (GPTMS). A significant effort is devoted to the characterization of the changes taking place at the PSi surface during functionalization. Moreover, we point at the biofunctionality of the GPTMS capping process by performing a selective plasma etching step, followed by the application of an immune assay.

2. Experimental

2.1. Preparation of PSi

The back side of p-type boron-doped (resistivity 0.05–0.1 $\Omega\cdot\text{cm}$) (100) oriented Si wafers were first coated with an aluminum layer to provide low resistance ohmic electrical contacts. They were subsequently cut into 15 mm \times 15 mm pieces and mounted into the sample holder. PSi was then formed by electrochemical etch of the silicon wafers in an aqueous electrolyte composed of a mixture of hydrofluoric acid (HF) (40%) and absolute ethanol (98%) (volume ratio 1:1). The current density was fixed at 80 mA/cm², and the anodization time at 20s, leading to a 1 μm thick film. PSi particles were also formed by applying fixed current density of 78 mA/cm² and periodically (every 50s) pulsed for 1s to a higher value (104 mA/cm²). The waveform was repeated for 30 cycles, producing highly porous and mechanically fragile layers spaced at predetermined points in the porous film [23]. The thickness induced instability of the PSi/Si interface causes a fragmentation of the layer, which can be easily scrapped from the surface. The introduced artificial cleavage planes allowed extracting PSi particles used for FTIR and SSNMR characterization.

2.2. Functionalization of the surface

Epoxy capped PSi structures were synthesized using GPTMS (Sigma Aldrich). The organosilane-based solution was prepared by diluting GPTMS in MeOH (0,2 % v/v) and the PSi films and particles were incubated in this solution for 30min, 1h, 2h and 3h, under visible light (150 W halogen lamp with maximum of 10 % power emission at 700 nm and power emission below 2% for radiation under 360 nm). The silane concentration used was selected to remain in the submonolayer regime and minimize homogeneous silanization reactions with solvent moisture. The samples were then cleaned by rinsing in methanol and dried under N₂ atmosphere. The whole process was carried out in a glove box.

2.3. Plasma etching

The selective plasma etching of GPTMS capped PSi was carried out in a capacitively coupled plasma using a laser machined 200 μm thick Si mask for patterning. The samples were loaded in a vacuum chamber equipped with an RF plasma system (R301, 13,56 MHz, 300 W maximal power) and a roots pump reaching $5 \cdot 10^{-2}$ Torr background pressure. A 5 min treatment at 50 W power with 30 sccm Ar ($5 \cdot 10^{-1}$ Torr) plasma was then performed. After etching, the Ar flow was cut, the background pressure reached and the chamber vented under N_2 . The Si mask was removed and the patterned GPTMS capped PSi used without further treatment.

2.4. Selective adhesion assays

We performed two different assays in order to demonstrate the adhesion selectivity of the plasma processed contrasts: a) using activated colloidal Au nanoparticles (GNPs) and b) through an immune assay. The first one consisted in incubating the GPTMS micropatterned PSi in a $-\text{COOH}$ terminated GNPs solution (5 $\mu\text{g/mL}$ in PBS) for 1h at 37°C , and the further optoplasmonic detection of the GNPs bound to the surface by using dark field optical microscopy (Nikon Eclipse Ni). The second experiment involves non-specific binding of proteins from mouse serum with the GPTMS groups and their detection with fluorescently labelled goat-antimouse antibody without previous blocking. We diluted the mouse serum in PBS (1/100) and we deposited the samples upside down on droplets of 50 μL for 1h. After rinsing the sample with PBS for three times we incubated the fluorescently labelled antibody diluted in PBS in the dark. The samples were then cleaned with PBS, water and EtOH to eliminate any un-specifically adsorbed antibody. The surfaces were observed in an inverted Fluorescence microscope (Olympus) equipped with a CCD camera.

2.5. Characterization

Field emission SEM images from PSi surfaces were obtained in a Philips XL30S microscope operated at 10 keV. Water contact angles (WCAs) were measured in the sessile drop configuration using a KSV 100 goniometer, droplets of 3 μ l and 5 different measurements on independent areas for statistical purposes. XPS measurements were carried out with a SPECS GmbH photoelectron spectrometer with energy analyzer PHOIBOS 150 9MCD. XPS spectra were recorded using non-monochromatic Mg K_{α} excitation at pass energies of 75 eV for survey and 25 eV for high-resolution core-level spectra. The electron emission angle was 0° and the source-to-analyzer angle was 90°. The data were processed using CasaXPS v16R1 (Casa Software, UK).

The vibrational spectroscopy characterization of the functionalized PSi particles was performed by FTIR using a Bruker Vector 22 (resolution 8 cm^{-1} , 4000-400 cm^{-1} , 32 scans at 10 kHz) in transmission configuration after preparation of KBr disks. SS-NMR spectra were recorded with a Bruker AV-400-WB equipped with a 4 mm triple probe channel using ZrO rotors (10 kHz). A cross-polarization (CP-MAS) pulse sequence was used between ^1H and ^{13}C with dipolar decoupling of ^1H at 80 kHz. The work frequencies were 400.13 MHz for ^1H and 100.61 MHz for ^{13}C . The spectral width was 35 KHz, the ^1H excitation pulse 2.75 μs , the contact time 3 ms, the relaxation time 4s and 1k scans were accumulated. Adamantano (CH_2 29,5 ppm) was used as secondary reference relative to TMS as primary reference. For the ^{29}Si CP/MAS experiment, a ^1H excitation pulse of 3 μs was used ($\pi/2$). The spectral width was 40 kHz and the relaxation time 5s. Caolin (-91,2 ppm) was used as secondary reference relative to TMS as primary reference. SS-NMR analysis by $^1\text{H} \rightarrow ^{29}\text{Si}$ CP/MAS is a surface selective technique favoring the detection of ^{29}Si at the surface. Indeed, the combination of cross polarization (CP) with magic angle spinning (MAS) enhances NMR sensitivity and resolution [24][25].

3. Results and discussion

3.1 GPTMS capping of PSi layers

The efficiency of the functionalization of PSi layers with GPTMS was studied by XPS. The survey spectrum from a GPTMS layer functionalized during 3 h evidenced the presence of C (28.8 at %), O (19.6 at %), Si (51.2 at. %) and F species (0.5 at. %) on the surfaces (F as a trace of PSi anodization process). A more detailed insight into chemical binding state and available surface species is provided by core level C 1s and Si 2p spectra. Figure 1 shows a deconvolution analysis of the corresponding C 1s and Si 2p spectra, which allows identifying the contributions of the different types of covalent bonds. Regarding the C 1s spectrum (Fig. 1a), in addition to the alkyl-related C-C/C-H component (C1) at 285.11 eV, a second component located at 286.63 eV is found that is assigned to C-O bonds of the epoxy and ether moieties (C2) of the GPTMS molecule [26,27], strongly suggesting the attachment of a GPTMS layer on the PSi surface. However, the measured peak area component ratio C1:C2 is very high (~ 4) compared with the ratio expected for a complete reaction [27], which suggests a submonolayer regime for the GPTMS capping process. In the case of the Si 2p core level (fig. 1.b), both elemental Si and Si oxide peaks were observed at 99.9 (Si1) and 103.0 eV (Si2), respectively. The Si oxide peak is due to oxidation of Si during activation with visible light by using residual moisture as reactant [28] and to the Si-O bonds from GPTMS [29]]. By plotting the evolution of the Si1/Si2 peak area ratio along visible light activation time, a linear increase is observed, suggesting the visible light promotion of the PSi oxidation and GPTMS binding.

3.2 Surface morphology

The microstructure of PSi, dependent on processing parameters and Si wafer properties, was studied by SEM. Figure 2 shows the morphological comparison between the pristine PSi (Fig. 2a) and the GPTMS functionalized PSi (Fig. 2b). Wide fields are selected to identify the

homogeneity of the surface at the scales where the pores start to be observable, while insets show a higher magnification view of the columnar pore structure and its homogeneous distribution. We can note the similarity between the pristine PSi and the functionalized structure. In particular, there is no film or colloidal structure associated to the organosilane modification that can obstruct the pores. This result supports that the modification takes place through a mild heterogeneous assembly of the organosilane, which does not lead to adsorbed structures issuing from a previous (in liquid) homogeneous nucleation. The light activated process gives thus rise to a GPTMS assembly with no identifiable topographic structure.

3.3 Surface bound GPTMS on PSi particles

In order to deepen into the molecular structure of the GPTMS capping, we performed a FTIR spectroscopy study on PSi particles, which allow enhancing the surface signal. Figure 3 shows the FTIR spectra of pristine PSi and GPTMS functionalized PSi. In the former, the presence of the SiH_x species on the surface of the freshly-etched PSi is well evidenced [25]. Indeed, we can clearly distinguish the scissoring modes at 624, 662 and 901 cm^{-1} and, on the other hand, the stretching modes at 2085 and 2108 cm^{-1} [30]. After functionalization, the peaks corresponding to SiH_x modes remain partially present, suggesting that the surface has been only partially transformed upon the photo-assisted assembly. One can confirm the effective light activated oxidation of PSi through bands at 940-977 cm^{-1} ($\delta(-\text{O}_y\text{Si}-\text{H}_x)$) and 2195-2249 cm^{-1} ($\nu(-\text{O}_y\text{Si}-\text{H}_x)$). Additionally, we observe the presence of new peaks due to the aliphatic carbon chain at 575, 1318, 1382, 1472, 2849 and 2917 cm^{-1} corresponding to $\text{CH}_3\text{-C}$, $\delta_s(\text{CH}_3)$, $-\text{CH}_2-$, $\delta_{\text{AS}}(\text{CH}_3)$, $\nu_s(\text{CH}_2)$ and $\nu_{\text{AS}}(\text{CH}_2)$, respectively. Moreover, characteristic IR absorption bands of the GPTMS can be observed at 948 (asymmetrical ring stretching) and 800 cm^{-1} . The expected band corresponding to ring breathing at 1260-1240 cm^{-1} is not observed, certainly

because of the overlapping with the strong Si-O-Si absorption band. The absence of the diol vibration bands at 4080 cm^{-1} proved that the epoxide ring did not open forming diols [31].

The overlapping of some characteristic bands in the FTIR spectra makes the univocal identification of GPTMS difficult. In order to overcome this issue, we used SSNMR spectroscopy and assigned the peaks on the basis of the correlation of the chemical shifts with those observed on functionalized silicates [31-37]. Figure 4a shows the ^{29}Si NMR spectra of the GPTMS-functionalized PSi compared with freshly formed PSi. In the first one, the chemical shift of the dominant signal is centered at -96 ppm , with a line width (full width at half maximum, FWHM) of 20 ppm , which can be assigned to SiH or SiH₂ structural elements [32]. No signal corresponding to amorphous silicon (*a*-Si) (a very broad signal centered at -40 ppm) is seen. After functionalization, several peaks appear indicating the presence of different types of siloxane environments, which complement the signal of the underlying PSi. Indeed, the spectra exhibit peaks at -50 , -63 and -67 ppm assigned to the Si atoms covalently bonded to the organic group (T^1 [(SiO)Si(OMe)₂(CH₂CH₂CH₂OCH₂CH(O)CH₂)], T^2 [(SiO)₂Si(OMe)(CH₂CH₂CH₂OCH₂CH(O)CH₂)] and T^3 [(SiO)₃Si(CH₂CH₂CH₂OCH₂CH(O)CH₂)] respectively), confirming the reaction with the silane.

As the electronic shielding of the central Si increases, the chemical shift becomes increasingly negative with each additional Si-O-Si linkage [33]. It is remarkable that the dominant intensity is observed at T1, which would indicate that the organosilane is not fully condensed. This type of information on the reactivity at the surface is extremely relevant and cannot be extracted by using traditional spectroscopic techniques used for surface characterization of organosilanes such as XPS.

In addition, the peaks at -85 , -101 and -109 ppm correspond to germinal hydroxyl silanol sites [(O)₂Si(OH)₂, Q²], hydroxyl containing silicon sites [(O)₃SiOH, Q³] and cross-linked Si [(O)₄Si, Q⁴], respectively [24]. The high intensity of these peaks indicates that a significant part

of the PSi surface is oxidized to form Q^n structures, further illustrating the effectiveness of visible light in the surface oxidation of PSi particles. Figure 4b presents the ^{13}C carbon spectra of the organosilane functionalized PSi. The methylene carbons of the epoxide ring show resonances at 60,4 and 50,4 ppm, respectively, whereas the two oxymethylene chain carbon peaks appear at 72.8 ppm. The peak at 50.4 ppm also corresponds to the unreacted methoxy groups. Finally, the peak at 17.6 corresponds to the aliphatic chain [31].

Combining the results obtained from XPS, FTIR and SSNMR spectra, the overall information is consistent with the oxidation of the PSi surface and formation of the GPTMS layer. It appears however that the ratio of organosilane molecule with three siloxane bonds saturated to the PSi surface is low, which could support the evidence of the submonolayer functionalization of PSi.

3.4 Plasma patterning of GPTMS capped PSi

Figure 5a shows a low magnification SEM image of a GPTMS functionalized PSi surface after the selective treatment by the Ar plasma. We observe that the plasma treatment induces a change of the surface susceptibility to electron scattering, which perfectly reveals the selectivity imposed by the Si mask used during the process. In order to visualize the effects of the plasma treatment on the surface free energy, we carried out measurements of WCA at different steps of the surface micropatterning process (Fig 5b). The surface of the pristine PSi exhibits a hydrophobic behavior with WCA of 110° , which turned into a slightly hydrophilic surface after GPTMS capping (85°). Finally, the etching of the surface with the Ar plasma induces a superhydrophilic transition with WCA of 10° . A translation of these measurements to the micropatterned structures would imply WCA contrasts of 75° between the GPTMS areas (protected by the Si mask) and the Ar plasma exposed areas.

The spatially controlled plasma exposure allows achieving site-specific chemical modification. The resulting chemical and morphological contrast between exposed and non-irradiated regions can be used to control the assembly process of specific targets onto the activated areas. We performed two different assays in order to demonstrate the effect of these chemical and morphological contrasts on the interaction with biological matter and colloidal particles. The first experiment consisted in incubating the GPTMS patterned PSi sample in a –COOH terminated GNPs solution and the further optoplasmonic detection of the GNPs bound to the surface. The different possible final configurations for the chemical bonding of the GNPs is shown in Fig 6a. One is the ester of the primary hydroxyl group, and the second, the ester of the secondary hydroxyl group. The dark-field optical microscopy images of the final distribution of the GNPs are shown in Fig. 6b. We can observe that the GNPs are preferentially bound on the non-treated area of the GPTMS capped surface (interconnected squares), identified by the randomly localized red colored scattering induced by the plasmonic effects on the GNPs.

Then, we performed an experiment involving non-specific interaction of the GPTMS micropatterned PSi surface with proteins of mouse serum and their detection with a fluorescently labelled goat-antimouse antibody without previous blocking. Fig 6c shows the green filtered fluorescence microscope images after the immune reaction. It can be seen that the dominant green fluorescence from the antibody colocalizes with the GPTMS capped areas (interconnected squares). Moreover, red fluorescence images were recorded as internal control. We could observe that the Ar plasma exposed area presents more red autofluorescence, typical of PSi[38], clearly indicating a thinner a bio-organic absorption layer with respect to the GPTMS capped areas.

4. Conclusions

A visible light activated process has been proposed for the synthesis of GPTMS functionalized PSi structures at low concentrations of 0.2%. Light activation is shown to catalyze the oxidation of PSi making viable a reaction with organosilane, normally requiring a previous thermal or chemical oxidation. The process leads to a homogeneous surface with no traces of oligomerized silane structures, which suggest that organosilane coverage is below one monolayer and makes the process useful as model for the analysis of organosilane-PSi interfaces. The observations made by SS-NMR complemented those made by FTIR and XPS. Indeed, by using ^{13}C SS-NMR one can differentiate aliphatic chain carbons, which is not feasible by surface spectroscopic techniques. The use of ^{29}Si SS-NMR has been useful in the determination of GPTMS binding efficiency, which is quite low in view of the dominant T1 peak among the peaks corresponding to the ^{29}Si from the bound GPTMS.

An Ar plasma treatment through a Si mask confirmed that GPTMS-PSi surface free energy contrasts could be created. Their functionality was put in evidence through a colloidal optoplasmonic approach using activated GNPs a fluorescence immunoassay. The advantage of plasma modification is that the surface properties can be enhanced selectively, while the bulk attributes of the materials remain unchanged. The ability to control the composition and reactivity of GPTMS, combined with simple methods to create micropatterns, makes this class of surfaces a good choice for fundamental mechanistic studies of protein adsorption and cell adhesion.

Acknowledgments

Authors thank L. García Pelayo for his technical assistance during materials processing and M.J. de la Mata Segarra for acquisition of the SS-NMR spectra. We acknowledge MSC funding provided by the European Commission through FPVII grant THINFACE (ITN GA 607232).

References

- [1] Y.A. Badr, K.M. Abd El-Kader, R.M. Khafagy, Raman spectroscopic study of CdS, PVA composite film, *J. Appl. Polym. Sci.* 92 (2004) 1984-1992.
- [2] L. Sacarescu, G. Roman, G. Sacarescu, M. Simionescu, Fluorescence detection system based on silicon quantum dots - polysilane nanocomposites, *eXPRESS Polymer Letters*. 10 (2016) 990-1002.
- [3] E. Makila, L.M. Bimbo, M. Kaasalainen, B. Herranz, A.J. Airaksinen, M. Heinonen, E. Kukk, J. Hirvonen, H.A. Santos, J. Salonen, Amine modification of thermally carbonized porous silicon with silane coupling chemistry, *Langmuir*. 28 (2012) 14045-14054.
- [4] A. Munoz Noval, V. Sanchez Vaquero, E. Punzon Quijorna, V. Torres Costa, D. Gallach Perez, L. Gonzalez Mendez, I. Montero, R.J. Martin Palma, C. Climent Font, J.P. Garcia Ruiz, M. Manso Silvan, Aging of porous silicon in physiological conditions: Cell adhesion modes on scaled 1D micropatterns, *Journal of Biomedical Materials Research A*. 100 (2012) 1615-1622.
- [5] A. Munoz-Noval, V. Sanchez-Vaquero, V. Torres-Costa, D. Gallach, V. Ferro-Llanos, J.J. Serrano, M. Manso-Silvan, J.P. Garcia-Ruiz, F. del Pozo, R.J. Martin-Palma, Hybrid luminescent/magnetic nanostructured porous silicon particles for biomedical applications, *Journal of Biomedical Optics*. 16 (2011).
- [6] H. Kao, C. Liao, T. Hung, Y. Pan, A.S.T. Chiang, Direct synthesis and solid-state NMR characterization of cubic mesoporous silica SBA-1 functionalized with phenyl groups, *Chem. Mater.* 20 (2008) 2412-2422. doi:10.1021/cm800147z.
- [7] L.A. DeLouise, B.L. Miller, Quantitative assessment of enzyme immobilization capacity in porous silicon, *Analytical Chemistry*. 76 (2004) 6915-6920. doi:10.1021/ac0488208.
- [8] H. Föll, M. Christophersen, J. Carstensen, G. Hasse, Formation and application of porous silicon, *Materials Science and Engineering R*. 280 (2002) 1-49. doi:10.1149/1.2134015.

- [9] Q.Y. Sun, L. de Smet, B. van Lagen, M. Giesbers, P.C. Thüne, J. van Engelenburg, F. de Wolf, H. Zuilhof, E. Sudhölter, Covalently attached monolayers on crystalline hydrogen-terminated silicon: extremely mild attachment by visible light, *Journal of American Chemical Society*. 127 (2005) 2514-2523. doi:10.1021/ja045359s.
- [10] H. Sano, H. Maeda, S. Matsuoka, K.H. Lee, K. Murase, H. Sugimura, Self-assembled monolayers directly attached to silicon substrates formed from 1- hexadecene by thermal, ultraviolet, and visible light activation methods, *Japanese Journal of Applied Physics*. 47 (2008) 5659-5664. doi:10.1143/JJAP.47.5659.
- [11] J. Dong, A. Wang, K.Y. Simon Ng, G. Mao, Self-assembly of octadecyltrichlorosilane monolayers on silicon-based substrates by chemical vapor deposition, *Thin Solid Films*. 515 (2006) 2116-2122. doi:10.1016/j.tsf.2006.07.041.
- [12] N. Naveas, V. Torres Costa, D. Gallach, J. Hernandez-Montelongo, R.J. Martín Palma, J.P. Garcia-Ruiz, M. Manso-Silván, Chemical stabilization of porous silicon for enhanced biofunctionalization with immunoglobulin, *Sci. Technol. Adv. Mater*. 13 (2012) 045009.
- [13] K. Fukami, H. Tanaka, M.L. Chourou, T. Sakka, Y.H. Ogata, Filling of mesoporous silicon with copper by electrodeposition from an aqueous solution, *Electrochim. Acta*. 54 (2009) 2197-2202.
- [14] C. Mateo, R. Torres, G. Fernández-Lorente, C. Ortiz, M. Fuentes, A. Hidalgo, F. López-Gallego, O. Abian, J.M. Palomo, L. Betancor, B.C.C. Pessela, J.M. Guisan, R. Fernández-Lafuente, Epoxy-amino groups: a new tool for improved immobilization of proteins by the epoxy method, *Biomacromolecules*. 4 (2003) 772-777. doi:10.1021/bm0257661.
- [15] E. Punzon-Quijorna, V. Sanchez-Vaquero, A.M. Noval, D.G. Perez, A.C. Font, G. Ceccone, R. Gago, J.P.G. Ruiz, M. Manso Silvan, Optimized allylamine deposition for improved pluripotential cell culture, *Vacuum*. 85 (2011) 1071-1075.

- [16] S. Kurosawa, N. Kamo, T. Arimura, A. Sekiya, M. Muratsugu, Close-packed adsorption of F(AB')(2) fragment of immunoglobulin-G on plasma-polymerized allylamine film, *Japanese Journal of Applied Physics Part 1-Regular Papers Short Notes & Review Papers*. 34 (1995) 3925-3929.
- [17] Z.Y. Cheng, S.H. Teoh, Surface modification of ultra thin poly (epsilon-caprolactone) films using acrylic acid and collagen, *Biomaterials*. 25 (2004) 1991-2001.
- [18] M. Manso, P. Rossini, I. Malerba, A. Valsesia, L. Gribaldo, G. Ceccone, F. Rossi, Combination of ion beam stabilisation, plasma etching and plasma deposition for the development of tissue engineering micropatterned supports, *Journal of Biomaterials Science-Polymer Edition*. 15 (2004) 161-172.
- [19] Y. Zhang, K.L. Tan, B.Y. Liaw, D.J. Liaw, E.T. Kang, K.G. Neoh, Thermal imidization of fluorinated poly(amic acid)s on Si(100) surfaces modified by plasma polymerization and deposition of glycidyl methacrylate, *Langmuir*. 17 (2001) 2265-2274.
- [20] C. Padeste, P. Farquet, C. Potzner, H.H. Solak, Nanostructured bio-functional polymer brushes, *Journal of Biomaterials Science-Polymer Edition*. 17 (2006) 1285-1300.
- [21] W.J. Dressick, J.M. Calvert, Patterning of self-assembled films using lithographic exposure tools, *Japanese Journal of Applied Physics Part 1-Regular Papers Brief Communications & Review Papers*. 32 (1993) 5829-5839.
- [22] M. Manso-Silvan, G. Ceccone, F. Rossi, Surface analysis of plasma-patterned biofunctional hybrid titanate-aminosilane xerogel films, *Journal of Colloid and Interface Science*. 275 (2004) 577-583.
- [23] Z. Qin, J. Joo, L. Gu, M.J. Sailor, Size control of porous silicon nanoparticles by electrochemical perforation etching, *Particles & Particle Systems Characterization*. 31 (2014) 252-256.

- [24] W.K. Chang, M.Y. Liao, K.K. Gleason, Characterization of porous silicon by solid-state nuclear magnetic resonance, *J. Phys, Chem.* 100 (1996) 19653-19658. doi:S0022-3654(96)01921-1.
- [25] R.A. Caylor, Towards the characterization of silicon surface: solid state nuclear magnetic resonance studies, Ph. D. thesis (Colorado State University). (2011).
- [26] C. Funk, P.M. Dietrich, T. Gross, H. Min, W. Unger, W. Weigel, Epoxy-functionalized surfaces for microarray applications: surface chemical analysis and fluorescence labeling of surface species, *Surface and interface analysis.* 44 (2012) 890-894.
- [27] C. Nietzold, P.M. Dietrich, S. Ivanov-Pankov, A. Lippitz, T. Gross, W. Weigel, W. Unger, Functional group quantification on epoxy surfaces by chemical derivatization (CD)-XPS, *Surface and Interface analysis.* 46 (2014) 668-672.
- [28] Y.H. Ogata, K. Kobayashi, M. Motoyama, Electrochemical metal deposition on silicon, *Current Opinion in Solid State & Materials Science.* 10 (2006) 163-172.
- [29] A. Wong, U.J. Krull, Surface characterization of 3-glycidyloxypropyltrimethoxysilane films on silicon-based substrates, *Analytical and Bioanalytical Chemistry.* 383 (2005) 187-200.
- [30] T. Tsuboi, T. Sakka, Y.H. Ogata, Structural study of porous silicon and its oxidized states by solid-state high-resolution ^{29}Si NMR spectroscopy, *Physical Review B.* 58 (1998) 13863-13869. doi:10.1103/PhysRevB.58.13863.
- [31] P. Innocenzi, G. Brusatin, M. Guglielmi, R. and Bertani, New synthetic route to (3-glycidoxypropyl)trimethoxysilane-based hybrid organic-inorganic materials, *Chem. Mater.* 11 (1999) 1672-1679. doi:10.1021/cm980734z.
- [32] T. Pietrab, A. Bifone, V.-. Koch, A.P. Alivisatos, A. Pines, ^{29}Si high resolution solid-state nuclear magnetic resonance spectroscopy of porous silicon, *Journal of non-crystalline solids.* 202 (1996) 68-76. doi:10.1016/0022-3093(96)00144-5.

- [33] S.G. Vasil'ev, V.I. Volkov, E.A. Tatarinova, A.M. Muzafarov, A Solid-State NMR investigation of MQ silicone copolymers, *Appl. Magn. Reson.* 44 (2013) 1015-1025. doi:10.1007/s00723-013-0456-8.
- [34] R.S. Ribeiro, R.A.S. San Gil, E.L.S. Lima, Application of ^{13}C and ^{29}Si MAS NMR to the surface characterization of a barbituric derivative anchored on silica, *Ann. Magn. Reson.* 3 (2004) 116-118.
- [35] S. Radi, N. Basbas, S. Tighadouini, M. Bacquet, S. Degoutin, F. Cazier, New Amine-Modified Silicas: Synthesis, Characterization and Its Use in the Cu(II)-Removal from Aqueous Solutions, *Progress in Nanotechnology and Nanomaterials.* 2 (2013) 108-116. doi:10.5963/PNN0204002.
- [36] H. Lu, Synthesis and characterization of amino-functionalized silica nanoparticles, *Colloid Journal.* 75 (2013) 311-318. doi:10.1134/S1061933X13030125.
- [37] S. Ando, R.K. Harris, U. Scheler, Fluorine-19 NMR of Solids Containing Both Fluorine and Hydrogen, *Encyclopedia of Nuclear Magnetic Resonance.* 9 (2002) 531-550.
- [38] C. Rodriguez, P. Laplace, D. Gallach-Perez, P. Pellacani, R.J. Martin-Palma, V. Torres-Costa, G. Ceccone, M.M. Silvan, Hydrophobic perfluoro-silane functionalization of porous silicon photoluminescent films and particles, *Applied Surface Science.* 380 (2016) 243-248.

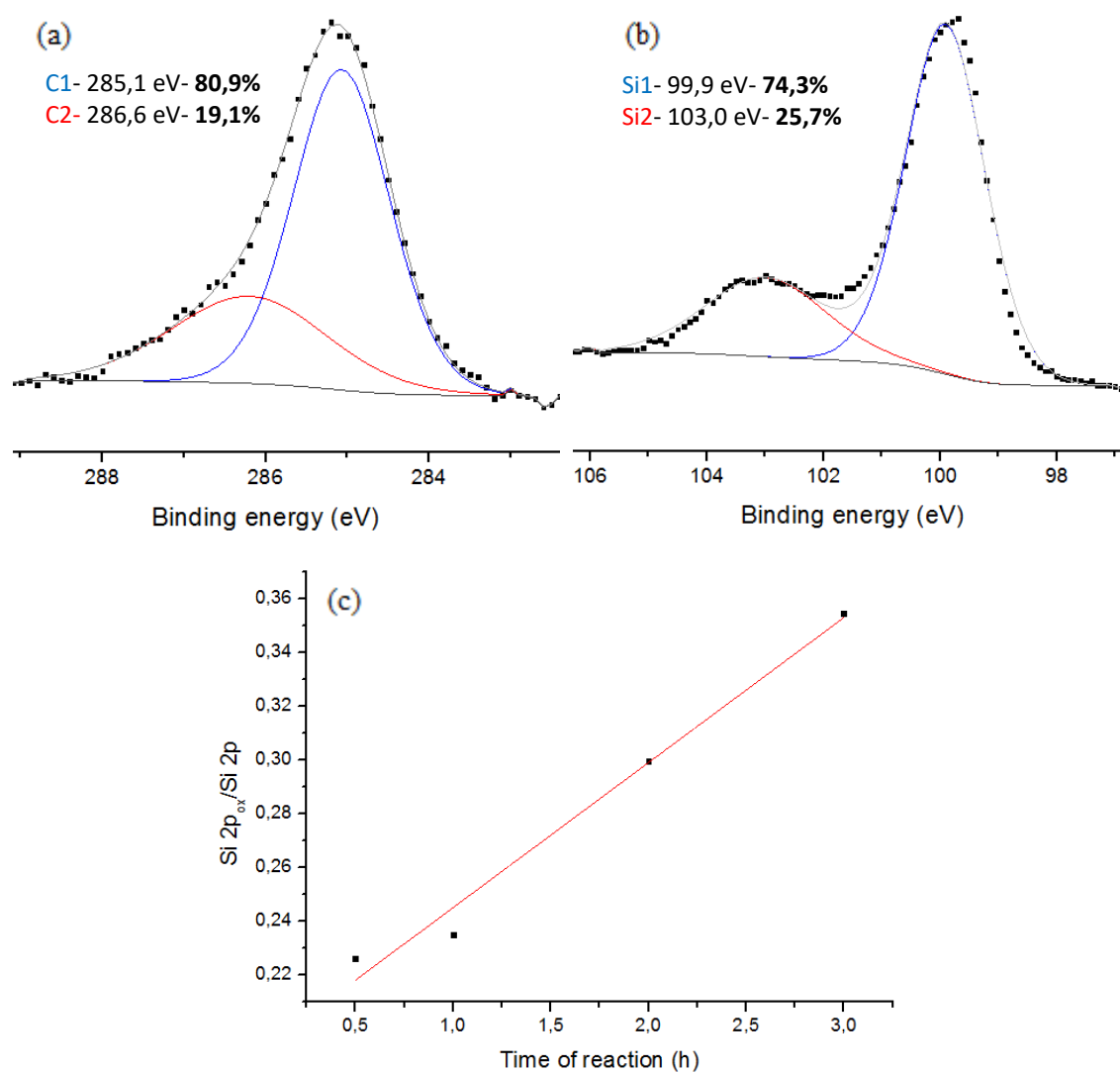


Figure 1. High resolution (a) C 1s and (b) Si 2p XPS spectra of GPTMS-capped PSi and (c) Si 2p_{ox}/Si 2p peak ratio as a function of visible light activation time.

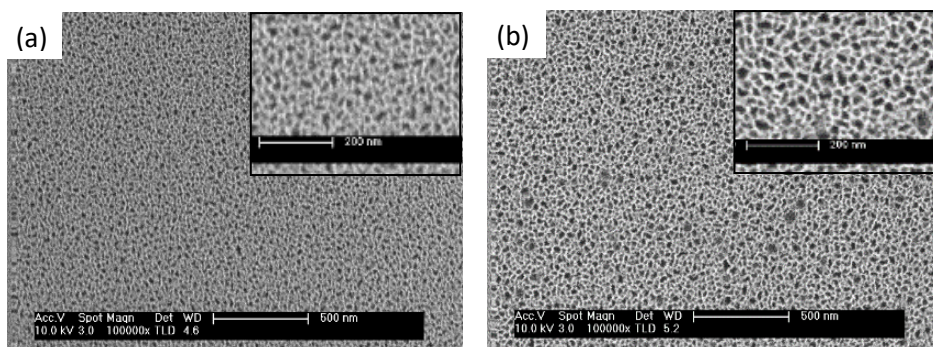


Figure 2. SEM images of the surface of (a) PSi and (b) PSi functionalized with GPTMS

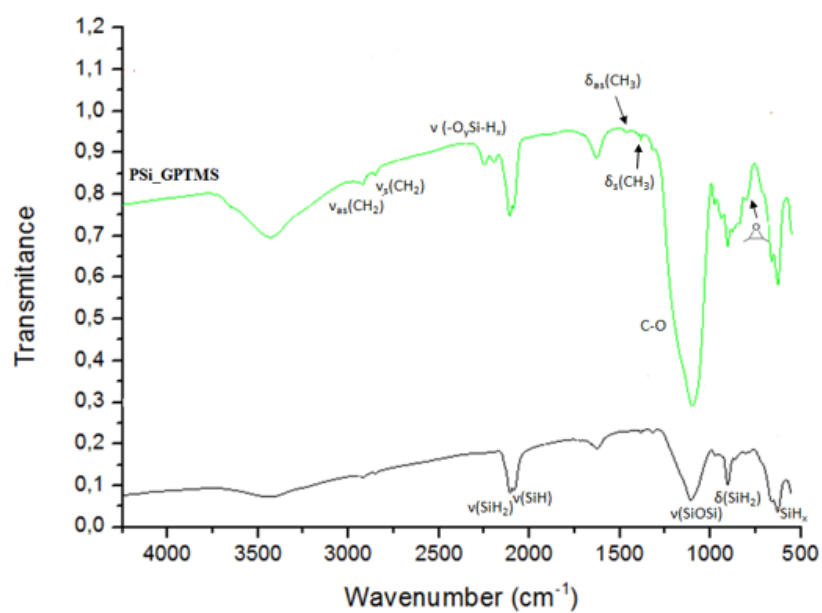


Figure 3. FTIR spectra of the GPTMS functionalized PSi particles compared with freshly formed PSi particles.

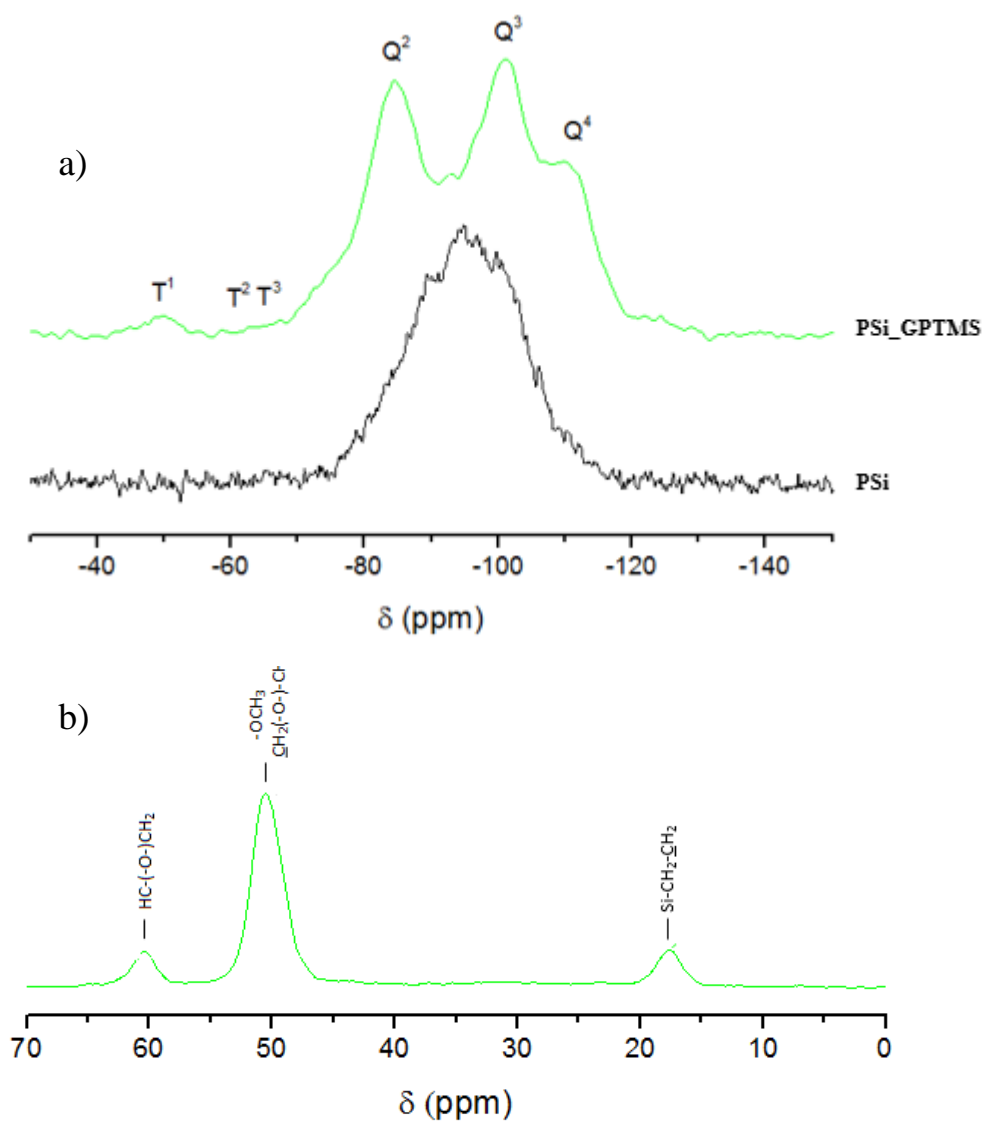


Figure 4. a) ^{29}Si NMR spectra of the organosilane functionalized PSi particles compared with the spectrum of freshly formed PSi particles. b) ^{13}C NMR spectrum of the PSi particles functionalized with GPTMS

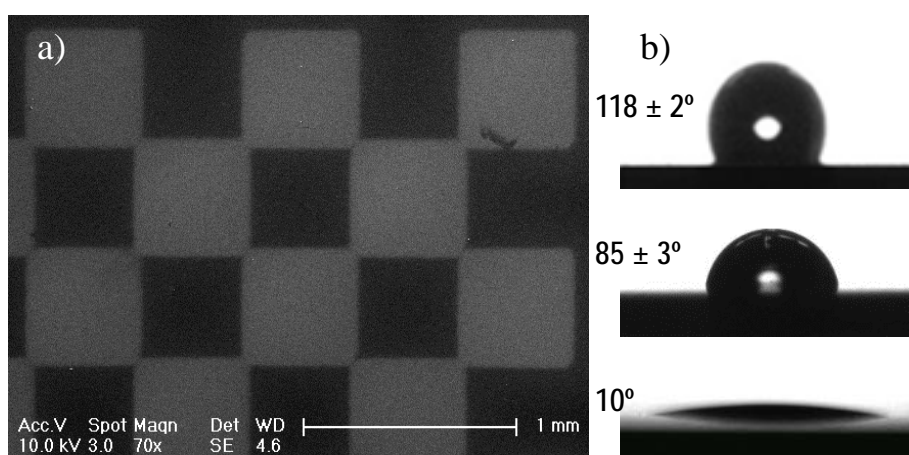


Figure 5. a) SEM images of the GPTMS/PSi micropattern created through the Si mask. b) Sequential transformation of static water contact angles for (from top to bottom) pristine PSi surfaces, GPTMS capped PSi, and plasma etched GPTMS capped Si.

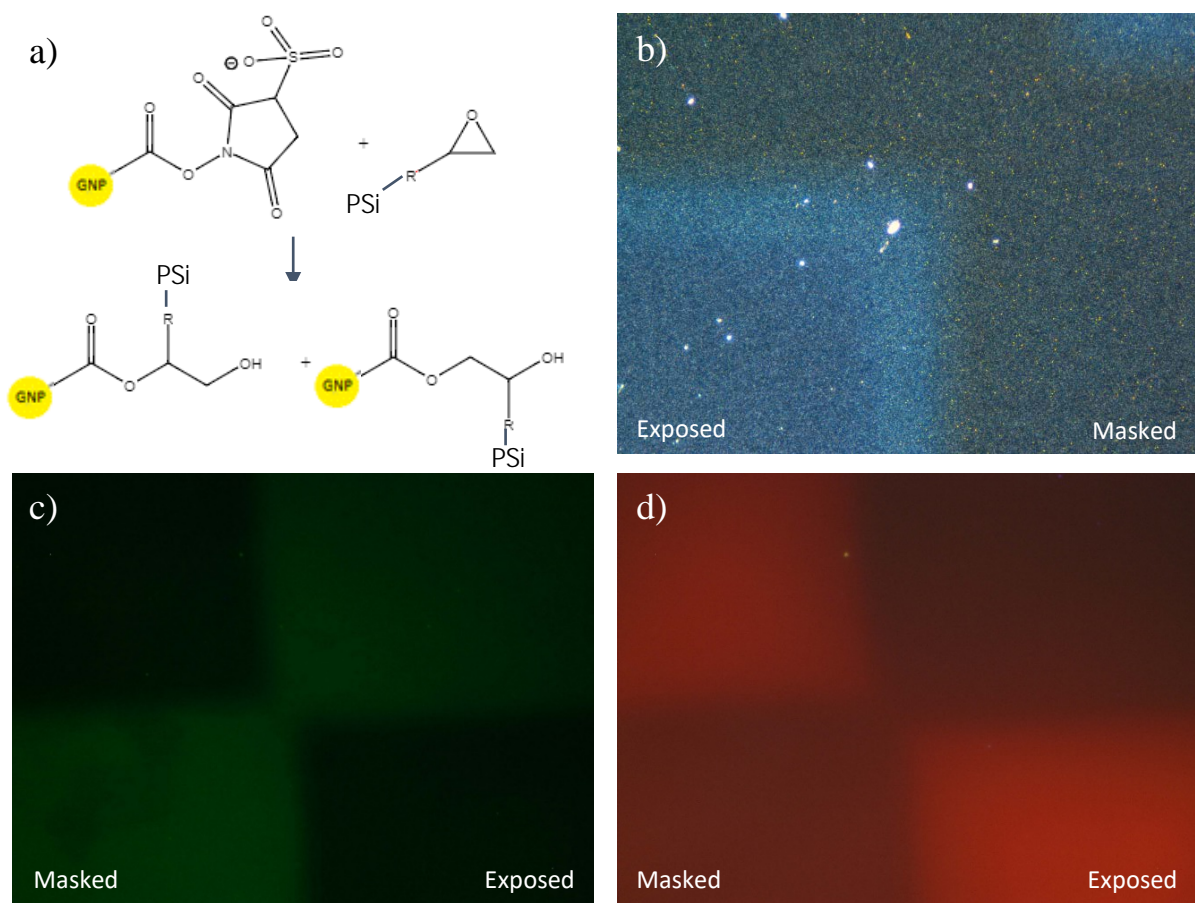


Figure 6. a) Reaction of the activated GNPs with the epoxy groups of the GPTMS. b) SEM images of the micropattern created through the mask. c) Dark-field images optoplasmonic detection. Fluorescence microscope images of the micropatterned GPTMS-functionalized PSi after mouse serum culture and goat anti mouse immune reaction with green d) and red e) filter.